29 April 1994

ELSEVIER

Chemical Physics Letters 221 (1994) 412–418

CHEMICAL PHYSICS LETTERS

Phonon-induced scattering between vibrations and multiphoton vibrational up-pumping in liquid solution

A. Tokmakoff [a], B. Sauter [a], A.S. Kwok [b], M.D. Fayer [a]

[a] *Department of Chemistry, Stanford University, Stanford, CA 94305, USA*

[b] *Hansen Experimental Physics Laboratory, Stanford University, Stanford, CA 94305, USA*

Received 20 December 1993; in final form 22 February 1994

Abstract

Fast phonon-induced scattering between an infrared active and a Raman active vibration in solution is investigated using picosecond infrared pump/anti-Stokes Raman probe experiments. Population from the infrared active T_{1u} CO stretching mode of tungsten hexacarbonyl in carbon tetrachloride at 1980 cm^{-1} scatters to the Raman active E_g mode at 2012 cm^{-1} but not to the A_{1g} mode at 2116 cm^{-1}. Equilibration occurs rapidly compared to the 700 ps population relaxation time. A power dependence of the line shape of the Raman mode indicates that significant population is pumped into high vibrational levels when high infrared pump powers are used.

1. Introduction

In this Letter, we report phonon-induced scattering between vibrational modes of the solute molecule, tungsten hexacarbonyl ($W(CO)_6$) in the solvent, carbon tetrachloride (CCl_4). Anti-Stokes and Stokes Raman spectra are recorded as a function of delay time following a picosecond infrared (IR) pulse that pumps the T_{1u} mode at 1980 cm^{-1}. In addition, the Raman spectra are studied as a function of IR pump power. Both experiments reveal novel aspects of the dynamics of vibrations in liquids. A knowledge of dynamic pathways and couplings is necessary to obtain a fundamental understanding of vibrational processes in liquids. Coupling between internal vibrational modes involves the instantaneous normal modes of the solvent, here referred to as phonons. Recently there has been considerable theoretical interest in the spectra of the low frequency phonon modes of liquids [1,2]. The results reported here suggest that the details of the low frequency liquid density of states play an intimate role in the dynamics of internal vibrational degrees of freedom.

Technological advances in the generation of fast IR pulses have provided a wealth of data on the vibrational relaxation of high frequency modes [3–8]. Coupling between high frequency vibrational modes has been observed with transient IR absorption and picosecond Raman spectroscopies [9–12]. Recent temperature-dependent studies of vibrational relaxation in liquids offer insights into the role of phonons in vibrational relaxation [13].

Fig. 1 shows an energy level diagram of the CO stretching modes of $W(CO)_6$ in CCl_4. There are three closely spaced spectroscopic lines, the IR active and Raman inactive, triply degenerate, T_{1u} mode, and Raman active and IR inactive E_g (doubly degenerate) and A_{1g} (non-degenerate) modes. The Raman active modes lie to higher energy by splittings of 32 and 136 cm^{-1}, respectively. Pump–probe studies of the T_{1u} mode have revealed a long population relaxation time $\tau = 700$ ps [3,13,14]. Recent studies have

SSDI 0009-2614(94)00276-V

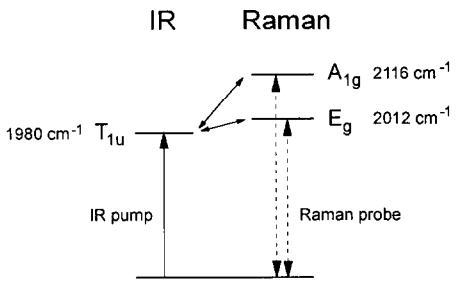

Fig. 1. Energy level diagram for the IR and Raman active CO stretching modes of $W(CO)_6$ in CCl_4 in the $\approx$2000 cm^{-1} spectral region. An IR pump pulse (solid arrow) populates the T_{1u} mode at 1980 cm^{-1}. A variably delayed visible pulse probes population scattering to the E_g and A_{1g} modes by anti-Stokes and Stokes Raman scattering (double headed dashed arrows).

observed a fast component ($<$2 ps) in the decay of this state, which was postulated to arise from phonon-induced scattering to the higher energy Raman modes [13]. This implies that population is exchanged between the IR and Raman modes quickly on the time scale of the overall population relaxation and that both the IR and Raman modes will decay with the same rate constant.

The coupling of infrared active modes has been observed in metal carbonyls with transient IR absorption spectra. After pumping the asymmetric CO stretches of $CO_4(CO)_{12}$ and $Rh(CO)_2(acac)$ in solution with a narrow band mid-IR pulse, a broad band mid-IR probe shows bleaching of the symmetric CO stretch [9]. The energy difference between the two modes is 9 cm^{-1} for $CO_4(CO)_{12}$ and 72 cm^{-1} for $Rh(CO)_2(acac)$ [9]. The decay constants for the pair of modes in each system are the same [10,15], consistent with a fast population exchange.

A picosecond IR pump/Raman probe experiment allows the dynamics of population redistribution to be probed between an IR active mode and a Raman active mode [11,12,16]. An IR active state is populated with an IR pump pulse, and redistribution of the population among Raman active modes is monitored by anti-Stokes scattering from a delayed visible probe pulse. In the experiments, the E_g mode (32 cm^{-1} higher in energy) is observed to be populated fast compared to the duration of the pulses. However, the A_{1g} mode (136 cm^{-1} higher in energy) is not populated. Identical observations are made for $W(CO)_6$ in $CHCl_3$ and $Cr(CO)_6$ in both CCl_4 and $CHCl_3$, and on $W(CO)_6$ in 2-methyltetrahydrofuran and 2-methylpentane. These experiments will be discussed in a subsequent publication [17]. The absence of the A_{1g} mode in the time delayed anti-Stokes spectrum can be explained by a cutoff energy in the phonon spectrum. In addition, it is found that when the IR pump power is increased, both the delayed Stokes and anti-Stokes spectra broaden and shift to the red. The broadening and shift can be fit to a model that has significant population in higher lying levels of the E_g mode. It is proposed that these are populated through multiple scattering events from the T_{1u} mode which is highly populated by intensive IR pumping. Multi-quanta excitation of the T_{1u} mode is also consistent with the non-exponential pump–probe decays of the T_{1u} mode observed at high pump powers [13].

2. Experimental

Infrared pump/Raman probe data were taken with picosecond mid-IR pulses generated with a $LiIO_3$ optical parametric amplifier (OPA). The laser system is a modified version of a system that is described elsewhere [18]. Briefly, the pulse train of a *Q*-switched, mode-locked, cavity-dumped Nd:YAG laser, with a 10% output coupler, is doubled and synchronously pumps a rhodamine B dye laser. The dye laser and the Nd:YAG laser are cavity-dumped simultaneously to form the idler and pump pulses for the OPA. The cavity-dumped pulse of the Nd:YAG laser is frequency-doubled (532 nm, 80 ps, 700 μJ), and the remaining fundamental light is also frequency-doubled to amplify the dye pulse in a single-stage double-pass amplifier, yielding tunable dye pulses of 40 ps, 45 μJ at $\approx$595 nm. The cavity-dumped pulse and the amplified dye pulse are made time coincident, and are mixed in a 30 mm $LiIO_3$ crystal generating 4 μJ, 40 ps pulses at $\lambda \approx 5.04$ μm with a 900 Hz repetition rate. The dye pulse energy is 60 μJ after amplification in the OPA. The bandwidth of the dye pulse was measured to be 1.3 cm^{-1}. The bandwidth of the dye and mid-IR were 1.3 cm^{-1}. The IR beam is focused to 160 μm diameter in the sample. The dye beam is sent down an optical delay line allowing up to 5 ns of delay and is focused to 100 μm. Timing between the two pulses was set by cross-

correlation of the IR and dye pulses in $LiLO_3$.

Data were taken on a 1×10^{-3} M solution of $W(CO)_6$ in CCl_4, corresponding to a mole fraction of $\approx 10^{-4}$ and a peak optical density of 0.9 using a 200 μm path length. The concentration is sufficiently low that Förster excitation transfer does not occur [3]. The absorption maximum of the T_{1u} CO stretch is 1980 cm^{-1}, with a 12 cm^{-1} bandwidth (fwhm). A Stokes Raman spectrum of the solution showed the E_g and A_{1g} lines to be centered at 2012 and 2116 cm^{-1}, respectively. Each has a 16 cm^{-1} bandwidth, and the relative intensity of the bands is 4:1.

The IR beam was tuned to the absorption maximum, corresponding to a dye wavelength of $\lambda = 594.76$ nm. The beams were brought into the sample in near-collinear geometry at 45° incidence to the sample cell with p-polarization. Incoherent Raman scattering was collected from the back face of the cell at 90° from the incident beams, using an $f = 1.2$ camera objective. The collected light was focused into a 0.25 m CCD spectrometer with 2 cm^{-1} resolution. Data was taken in 10 min collection periods, and several scans were averaged to obtain a final spectrum.

3. Results

Fig. 2a shows anti-Stokes Raman spectra of the region that contain both the E_g and A_{1g} CO stretching modes of $W(CO)_6$ in CCl_4. The E_g mode is observed with good intensity and signal-to-noise (S/N) ratio. The arrow indicates the location where the A_{1g} mode should appear. Given the S/N ratio and the ratio of the intensities of the Stokes lines, the A_{1g} mode should be visible even if it has only 10% of the population of the E_g mode. From the data it is clear that the E_g mode is populated following the IR pumping of the T_{1u} mode but the A_{1g} mode is not. Fig. 2b shows the E_g anti-Stokes spectrum as a function of delay time between the IR pump pulse and the dye probe pulse. The lines are highly asymmetric, and much broader than the equilibrium Stokes line. Furthermore, the line decays at a higher rate from the broadened low frequency side. The peak of the signal shifts by 8 cm^{-1} to higher frequency with increased delay, approaching the frequency of the equilibrium Stokes line.

Fig. 3 shows the integrated intensity of the anti-

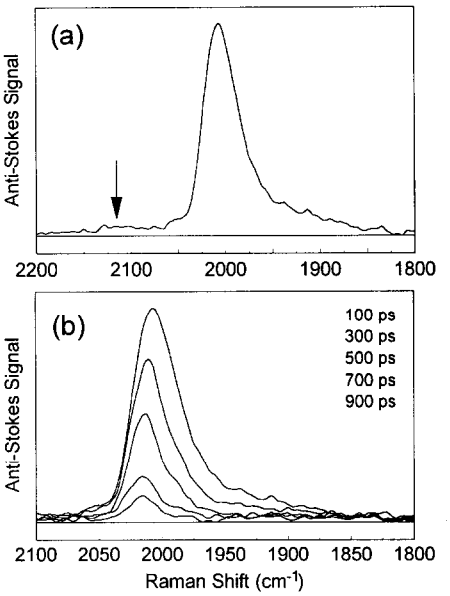

Fig. 2. (a) Anti-Stokes Raman spectrum of $W(CO)_6$ in CCl_4 taken 100 ps following IR pumping of the T_{1u} mode in the spectral range that includes the E_g and A_{1g} Raman active modes. The E_g mode is clearly visible demonstrating rapid population by phonon scattering from the IR pumped T_{1u} mode. The arrow marks the location where the A_{1g} mode should appear. Given the signal-to-noise ratio, the A_{1g} mode should be observable if it acquired any significant population. (b) Anti-Stokes Raman spectra of the E_g CO stretching mode as a function of delay time between the IR pump and the visible probe pulses. The peak is still visible 900 ps after pumping.

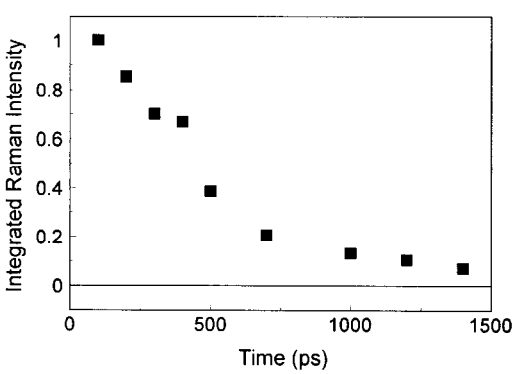

Fig. 3. Integrated intensities of the anti-Stokes Raman spectra of the E_g mode as a function of delay between the IR pump and the visible probe pulses. The decay is non-exponential.

Stokes Raman spectra as a function of delay time. The intensity clearly decays on an ≈ 500 ps time scale in a non-exponential manner. This decay is similar to the 700 ps decay observed for the relaxation rate of the $v=1$ level of the T_{1u} CO stretching vibration using single-color IR pump–probe experiments [3,13]. When the pump–probe experiments are conducted at sufficiently low fluence (<0.6 mJ/cm^2), the decays are single exponential [13]. However, at the high pump powers used for the experiments presented here, the pump–probe decays become non-exponential and the decay times change [13].

Anti-Stokes Raman spectra of the E_g mode with 100 ps delay between the pump and probe pulses were observed for $W(CO)_6$ in several other solvents. Similar spectra to those presented above were obtained for solutions of $W(CO)_6$ in $CHCl_3$, 2-methylpentane, and 2-methyltetrahydrofuran, as well as for $Cr(CO)_6$ in CCl_4 and in $CHCl_3$. No population was observed in the A_{1g} mode in any of these solutions.

The broadening of the low-frequency edge of the anti-Stokes spectra is consistent with the population of vibrational levels higher than $v=1$. Fig. 4 shows the pump power dependence of the line shape of the Stokes spectrum of the E_g mode. Spectra were taken with pump fluences of 15.0, 4.0, 1.25, and 0 mJ/cm^2, at a time delay of 100 ps between the IR pump and dye probe beam. The data show significant broadening to the low-frequency side of the line with increasing pump power. Also, the integrated areas of the spectra increase with pump power.

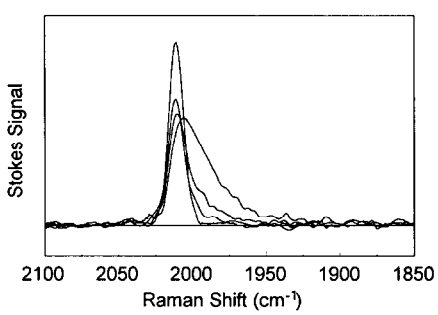

Fig. 4. IR pump power dependence of the E_g mode's Stokes line shape recorded 100 ps after IR pumping of the T_{1u} mode. The Stokes spectra were taken with IR pump fluences of (from top) 0, 1.25, 4.0, and 15.0 mJ/cm^2. The pulse duration was 40 ps, and the IR beam was focused to a 160 μm diameter.

4. Discussion

The appearance of population in the E_g mode directly after populating the T_{1u} mode, and the decay kinetics of the two modes that are essentially equivalent given the differences in the excitation powers used in the Raman and pump–probe experiments clearly demonstrates population equilibration between them that is much faster than the time scale for decay of population to the ground vibrational state. Population is exchanged quickly, so that the effective relaxation time of either of the modes involves the combined relaxation pathways out of both modes into the bath. In this case, the bath refers to low frequency intramolecular vibrations, solvent vibrations, or solvent phonons. Phonons scatter population between these two CO stretching modes on a time scale that is more than two orders of magnitude faster than the rate of vibrational energy flow out of the modes.

The reason for this disparity in rates of scattering and population relaxation is related to the energetics of the process. The rate of relaxation processes, described by Fermi's Golden Rule, are highly dependent on the order of the process and the occupation of the modes involved [13,19,20]. For the CO stretching vibration to depopulate, energy must be conserved. This can be accomplished by the excitation of lower frequency vibrations of the $W(CO)_6$ and the solvent. To conserve energy, it will probably be necessary to excite a phonon mode, since the phonons provide a continuum of low-frequency states which can make up the energy mismatch associated with a combination of vibrational modes. Relaxation of the CO stretching vibrations involves a high-order anharmonic process. These high-frequency vibrations are energetically isolated from the remaining bath modes. Solute and solvent vibrations have frequencies $\omega < 800$ cm^{-1} [21,22], and liquid phonons typically have frequencies $\omega < 150$ cm^{-1} [23]. Thus, a fifth-order anharmonic coupling matrix element, involving the annihilation of the CO stretch and the creation of three lower frequency vibrations and a phonon, will dominate the relaxation dynamics [13]. By nature, such high-order processes result in a slow relaxation. In contrast, scattering between the T_{1u} and the E_g modes can be accomplished by a cubic anharmonic process, by absorption of a 32 cm^{-1} phonon (scattering up in energy) or stimulated emission of a

32 cm^{-1} phonon (scattering down in energy). This phonon scattering mechanism is efficient both because it involves a low-order process and because the 32 cm^{-1} phonon is highly populated at room temperature.

The rate of phonon scattering between the T_{1u} and E_g modes can be estimated from pump–probe data and IR absorption spectra. Single color IR pump–probe experiments were conducted using the Stanford free electron laser which provides ≈ 2 ps pulses [13,24]. The experiments were performed on $W(CO)_6$ in CCl_4 with the probe pulse at the magic angle to eliminate a component in the decay from orientational relaxation. The decays were exponential except on the time scale of the pulse duration where a small deviation from exponentiality is observed. If the scattering time from the T_{1u} to the E_g mode, τ_s, is as slow as 2 ps, a distinct bi-exponential would be observed. On the other hand, if τ_s is much faster than 0.5 ps, no measurable response would appear in the data. The small deviation from exponentiality suggests a scattering time intermediate to these limits. Another indication of the scattering time can be based on the IR vibrational line width which is $\approx$ 13 cm^{-1}. If the line width, $\Delta\nu$, is determined completely by scattering out of the T_{1u} mode, then $\Delta\nu = 1/2\pi\tau_s$. This limits the scattering time to $\tau_s > 0.4$ ps. Based on these considerations, we estimate a scattering time of ≈ 1 ps.

It is clear from the data in Fig. 2a that there is no detectable population scattered into the higher energy A_{1g} mode. The fast scattering between the T_{1u} and E_g modes brings them into thermal equilibrium on a time scale fast compared to the vibrational lifetime. Although the A_{1g} mode is 136 cm^{-1} above the T_{1u} mode, based only on energetics, it should still be highly populated since $kT \approx 206$ cm^{-1} at room temperature. If the A_{1g} mode were also in thermal equilibrium, the ratio of the Boltzmann factors (and accounting for the degeneracy of the E_g mode) would make the A_{1g} population 30% of the E_g population. As discussed above, we would be able to detect the A_{1g} mode readily even it if had only 10% of the E_g population. This indicates that there is little scattering to the A_{1g} mode on the time scale of the vibrational lifetime (hundreds of picoseconds).

The lack of population in the A_{1g} mode suggests a certain structure of the phonon density of states of CCl_4. Efficient phonon scattering will occur for a cubic process involving one phonon. The lack of any significant population in the A_{1g} mode suggests that there are virtually no 136 cm^{-1} phonons in the liquid. Further, since there is substantial population in the E_g mode that could be scattered to the A_{1g} mode, the density of phonon states at 104 cm^{-1} must also be very small. This suggests that the phonon density of states has dropped approximately to zero by ≈ 100 cm^{-1} in CCl_4 but that there is substantial density of states at 32 cm^{-1}. Even if the phonon density of states cuts off below 104 cm^{-1}, population could still be scattered to the A_{1g} mode through a quartic (two-phonon) process. The rate of a two-phonon process will be greatly reduced compared to the one-phonon mechanism. Thus, the scattering would occur on a much longer time scale, and no substantial population would be transferred to the A_{1g} mode within the vibrational lifetime.

The possibility exists that the phonon density of states in CCl_4 is still significant above 104 cm^{-1}, yet the rate of scattering is much slower to the A_{1g} mode. This would occur if the magnitude of cubic coupling matrix elements for both the $T_{1u} \rightarrow A_{1g}$ and $E_g \rightarrow A_{1g}$ transitions are substantially less than that for the $T_{1u} \rightarrow E_g$ transition. For no Raman signal to be observed, the rate for scattering to the A_{1g} mode would have to be longer than T_1. This implies that the matrix elements for *both* $T_{1u} \rightarrow A_{1g}$ and $E_g \rightarrow A_{1g}$ would be smaller than the $T_{1u} \rightarrow E_g$ matrix element by a factor of 30–40.

Fig. 4 demonstrates pumping to high vibrational levels of the CO stretching modes of $W(CO)_6$ in CCl_4. The figure displays Stokes spectra of the E_g mode taken following pumping at various power levels of the IR active T_{1u} mode. A spectrum is shown for zero IR pump power. This is the normal ground state ($v=0$) spectrum of the E_g mode. As the IR pump power is increased, the spectrum shifts to the red and broadens substantially. As discussed above, when the T_{1u} mode is pumped, phonon scattering populates the E_g mode. This is clearly demonstrated by the appearance of the anti-Stokes spectrum. Population of the E_g mode will also change the Stokes spectrum. Transfer of population from $v=0$ to $v=1$ will result in Stokes scattering from $v=1$ to $v=2$. The anharmonicities of the T_{1u} and E_g modes are approximately 6 cm^{-1}, corresponding to a difference in the transition

frequency of 12 cm^{-1} between the $v=0\rightarrow1$ and $v=1\rightarrow2$ transitions [3,25–27]. Thus when population is put into higher levels of the E_g mode, new peaks appear each successively shifted to the red side of the $v=0$ Stokes line by ≈ 12 cm^{-1}. Since the shift is comparable to the line width, the peaks are not resolved but rather result in a broadening and shift of the peak of the envelope. Removing population from the $v=0$ level will also result in a reduction in the intensity of the $v=0$ to $v=1$ Stokes signal.

Under high pump power conditions, many quanta are absorbed by the T_{1u} mode. The Rabi frequencies are high for the pumping conditions used. For a pump energy of 3.7 μJ and the IR spot size used, the Rabi frequency is $\omega_1=15$ cm^{-1}. This is more than sufficient to overcome the anharmonicity and produce multiphoton up-pumping of the T_{1u} transition. In addition, the transition dipole matrix element, and therefore the Rabi frequency, scales as $\sqrt{v}$, where v is the quantum number of the vibrational level. This scaling helps offset the increased detuning of the laser from the higher level transitions. These conditions, as well as the inherently long population relaxation times, make efficient off-resonant pumping possible.

When the pump power is turned up, multiple quanta are absorbed by the IR active T_{1u} mode. This in turn, through phonon scattering, will produce high levels of excitation of the E_g mode. There are many path ways that can produce multiple excitations of the E_g mode. For example, a photon is absorbed and scattered to the E_g mode. Another photon is absorbed by the T_{1u} mode. Now both modes are singly excited. There is a cubic anharmonic process that annihilates the T_{1u} excitation, annihilates a phonon, and raises the level of excitation of the E_g mode from $v=1$ to $v=2$. Because of the anharmonicity of the vibration, this process requires a 20 cm^{-1} phonon, rather that a 32 cm^{-1} phonon. There are many other pathways that will populate the $v=2$ level of the E_g mode. With the E_g mode in $v=1$, the T_{1u} mode absorbs two photons and is in $v=2$. Again a cubic anharmonic process can result in the lowering of the T_{1u} mode to $v=1$, annihilation of a phonon, and raising the E_g mode from $v=1$ to $v=2$. This requires a 32 cm^{-1} phonon.

As more and more photons are absorbed by the T_{1u} mode, the E_g mode can be promoted to higher and higher levels of excitation. This is clearly shown by the increased broadening to the red and shift to the red of the Stokes spectrum as the IR pump power is increased. In addition to the shift and the broadening of the spectrum with increasing IR pump power, the integrated intensity of the spectrum actually increases. This arises because the Stokes Raman scattering matrix element contain a factor $\sqrt{v+1}$. The scattered intensity, which depends on the square of the matrix element, scales as $v+1$. Therefore, as high levels are populated, the integrated intensity increases, and the spectrum is very sensitive to the population of levels above $v=0$. By assuming that the line width of the $v=0\rightarrow1$ line (no IR pump) is the same for all of the higher level spectra and assuming a constant shift of each successive peak of 12 cm^{-1}, it is possible to fit the line shape and obtain an estimate of the relative populations of the occupied levels. Analysis of the data in Fig. 4 shows that at high pump powers there is significant population in modes shifted as much as 50 cm^{-1} from the $v=0\rightarrow1$ transition. These line shapes suggest population of states at least as high as $v=5$.

The significant population of the higher vibrational levels provides the reason for the non-exponential decay of the anti-Stokes Raman spectrum (Fig. 3). The integrated intensity of the line represents the total population in all anti-Stokes active vibrational levels. Since the contribution of these levels to the intensity of the Raman scattering scales as v and the relaxation rates of the levels are also expected to scale as v, the decay will be decidedly non-exponential. Population of high vibrational levels of the T_{1u} IR active mode is responsible for the non-exponential decays observed in pump–probe experiments conducted with high pump powers [3,13]. By analyzing the time dependence of the anti-Stokes and Stokes line shapes, it is possible to obtain the decay kinetics of the high lying vibrational levels. A detailed analysis of the power and time dependences of the line shapes and the pump–probe data will be presented subsequently [17].

5. Concluding remarks

Using IR pump/anti-Stokes Raman scattering probe experiments we have shown that phonon scattering rapidly populates the Raman active E_g mode of $W(CO)_6$ in CCl_4 following IR pumping of the T_{1u}

mode. Although the E_g mode, which is 32 cm^{-1} higher in energy than the T_{1u} mode, is efficiently populated by phonon scattering, the A_{1g} mode, 136 cm^{-1} to higher energy, is not. This suggests either a great decrease in the density of states of the CCl_4 phonons below ≈ 100 cm^{-1}, or the matrix elements for *both* scattering pathways to the A_{1g} mode are very small. Recent calculations of the density of states of CS_2 show a cutoff at ≈ 150 cm^{-1} [23]. Similar calculations for CCl_4 could help elucidate the reason for the lack of scattering to the A_{1g} mode.

Rapid scattering between vibrational levels is a source of homogeneous line broadening. Recently, IR vibrational photon echoes on the T_{1u} mode of $W(CO)_6$ in 2-methylpentane (2MP) were observed at room temperature [28], in contrast to photon echoes on $W(CO)_6$ in 2-methyltetrahydrofuran [8, 28] for which the echo decay became faster than the time resolution of the experiment (2 ps) at 140 K, about 50 K above the glass transition. Initial analysis of these experiments indicate that the observation of photon echoes in the room temperature 2MP liquid is associated with a relatively slow rate of scattering between the T_{1u} and E_g modes [28] in this solvent. Further experimental and theoretical investigations are aimed at elucidating the contribution of phonon-induced scattering to homogeneous vibrational line widths.

Acknowledgement

We would like to thank Dr. John Fourkas for very informative discussions pertaining to this work, and Professor Tom Keyes for providing us with calculations of the phonon density of states of CS_2. BS thanks the Alexander von Humboldt Foundation for a Feodor Lynen Fellowship. This work was supported by the National Science Foundation (DMR90-22675), the Office of Naval Research (N00014-92-J-1227-P02) and the Medical Free Electron Laser Program (N00014-91-C-0170).

References

[1] G. Seeley and T. Keyes, J. Chem. Phys. 91 (1989) 5581.
[2] B.-C. Xu and R.M. Stratt, J. Chem. Phys. 92 (1990) 1923.
[3] E.J. Heilweil, R.R. Cavanagh and J.C. Stephenson, Chem. Phys. Letters 134 (1987) 181.
[4] E.J. Heilweil, M.P. Casassa, R.R. Cavanaugh and J.C. Stephenson, Ann. Rev. Phys. Chem. 40 (1989) 143.
[5] H. Graener, Chem. Phys. Letters 165 (1990) 110.
[6] H. Graener and G. Seifert, J. Chem. Phys. 98 (1993) 36.
[7] H.J. Bakker, J. Chem. Phys. 98 (1993) 8496.
[8] D. Zimdars, A. Tokmakoff, S. Chen, S.R. Greenfield and M.D. Fayer, Phys. Rev. Letters 70 (1993) 2718.
[9] S.A. Angel, P.A. Hansen, E.J. Heilweil and J.C. Stephenson, Ultrafast phenomena, Vol. 7 (Springer, Berlin, 1990) p. 480.
[10] J.D. Beckerle, M.P. Casassa, R.R. Cavanagh, E.J. Heilweil and J.C. Stephenson, Chem. Phys. 160 (1992) 487.
[11] N.H. Gottfried and W. Kaiser, Chem. Phys. Letters 101 (1983) 331.
[12] J.R. Ambroseo and R.M. Hochstrasser, J. Chem. Phys. 89 (1988) 5956.
[13] A. Tokmakoff, B. Sauter and M.D. Fayer, J. Chem. Phys., in press.
[14] M. Iannone, B.R. Cowen, R. Diller, S. Maiti and R.M. Hochstrasser, Appl. Opt. 30 (1991) 5247.
[15] E.J. Heilweil, R.R. Cavanaugh and J.C. Stephenson, J. Chem. Phys. 89 (1988) 230.
[16] A. Laubereau and W. Kaiser, Rev. Mod. Phys. 50 (1978) 605.
[17] A. Tokmakoff, B. Sauter, A.S. Kwok and M.D. Fayer, in preparation (1993).
[18] A. Tokmakoff, C.D. Marshall and M.D. Fayer, J. Opt. Soc. Am. B 10 (1993) 1785.
[19] D.D. Dlott and M.D. Fayer, J. Chem. Phys. 92 (1990) 3798.
[20] A. Tokmakoff, M.D. Fayer and D.D. Dlott, J. Phys. Chem. 97 (1993) 1901.
[21] J.R. Madigan, J. Chem. Phys. 19 (1951) 119.
[22] J.P. Zietlow, F.F. Cleveland and A.G. Meister, J. Chem. Phys. 18 (1950) 1076.
[23] P. Moore and T. Keyes, J. Chem. Phys. (1993), submitted for publication.
[24] D.D. Dlott and M.D. Fayer, IEEE J. Quantum Electron. QE-27 (1991) 2697.
[25] L.H. Jones, Spectrochim. Acta 19 (1963) 329.
[26] D.M. Adams and I.D. Taylor, J. Chem. Soc. Faraday Trans. II 78 (1982) 1051.
[27] R.L. Amster, R.B. Hannan and M.C. Tobin, Spectrochim. Acta 19 (1963) 1489.
[28] A. Tokmakoff, D. Zimdars, B. Sauter, A.S. Kwok, R. Francis and M.D. Fayer, in preparation (1993).